Received: 4 July 2021 | Revised: 8 December 2021 | Accepted: 6 January 2022

DOI: 10.1111/psyp.14019

PSYCHOPHYSIOLOGY SPR WILEY

ORIGINAL ARTICLE

Neural correlates of unpredictable Stop and non-Stop cues in overt and imagined execution

Alberto González-Villar[1] | **Santiago Galdo-Álvarez**[2] | **María T. Carrillo-de-la-Peña**[3]

[1]Psychological Neuroscience Lab, CIPsi, School of Psychology, University of Minho, Braga, Portugal

[2]Department of Clinical Psychology and Psychobiology, University of Santiago de Compostela, Santiago de Compostela, Spain

[3]BaP (Brain and Pain) Lab, Department of Clinical Psychology and Psychobiology, University of Santiago de Compostela, Santiago de Compostela, Spain

Correspondence
María T. Carrillo-de-la-Peña, Departamento de Psicología Clinica y Psicobiología, Universidade de Santiago de Compostela, Santiago de Compostela, Spain.
Email: mteresa.carrillo@usc.es

Funding information
This work was supported by funding from the Galician Government (Consellería de Cultura, Educación e Ordenación Universitaria; Axudas para a consolidación e Estruturación de unidades de investigación competitivas do Sistema universitario de Galicia; grant number Ref:: ED431C 2021/04.); and from Fundação para a Ciência e a Tecnologia––Scientific Employment Stimulus (CEECIND/02639/2017 to A.G.V.)

Abstract

The ability to inhibit incorrect behaviors is crucial for survival. In real contexts, cues that require stopping usually appear intermixed with indications to continue the ongoing action. However, in the classical Stop-signal task (SST), the unpredictable stimuli are always signals that require inhibition. To understand the neural mechanisms activated by low-probability nonstop cues, we recorded the electroencephalography from 23 young volunteers while they performed a modified SST where the unpredictable stimuli could be either Stop or confirmatory Go signals (CGo). To isolate the influence of motor output, the SST was performed during overt and covert execution. We found that, paradoxically, CGo stimuli activated motor inhibition processes, and evoked patterns of brain activity similar to those obtained after Stop signals (N2/P3 event-related potentials and midfrontal theta power increase), though in lesser magnitude. These patterns were also observed during the imagined performance. Finally, applying machine learning procedures, we found that the brain activity evoked after CGo versus Stop signals can be classified above chance during both, overt and imagined execution. Our results provide evidence that unpredictable signals cause motor inhibition even when they require to continue an ongoing action.

1 | INTRODUCTION

One key aspect of human behavior is the ability to inhibit unwanted or erroneous movements, whose dysfunction is at the basis of certain psychiatric pathologies (Diamond, 2013). The Stop-signal task (SST) is commonly used to study reactive motor inhibition that is, stopping an ongoing action. During the SST, participants respond to a "Go" signal, while unpredictably the "Go" signal is followed by a "Stop" signal, indicating that the motor action must

be stopped. The Stop signal activates a cortical network including areas like the anterior insula, anterior cingulate cortex, inferior frontal cortex, or the presupplementary motor area (Aron, 2011; Swick et al., 2011; van Boxtel et al., 2005). The Stop signal is associated to two components of the event-related potentials (ERPs), Stop-N2 and Stop-P3, with maximum amplitude over midfrontal scalp locations. The Stop-N2 presumably reflects conflict monitoring, while the functional meaning of the Stop-P3 component is still controversial (Huster et al., 2013). Although Stop-P3 has been related to the engagement of inhibitory processes (Enriquez-Geppert et al., 2010; Wessel & Aron, 2015), it seems more likely that this component is related to post-inhibitory operations, such as performance monitoring (Huster et al., 2020; Skippen et al., 2020), since behavioral inhibition precedes the onset of P3. However, the fact that the amplitude of this component is greater for Stop signals than for other infrequent stimuli that do not require motor inhibition suggests that Stop-P3 does reflect processes that are specific for action-stopping (Tatz et al., 2021). In the time-frequency domain, stop signals are associated to increased mid-frontal theta power-related to conflict detection and the N2 component-, reduced posterior alpha power - related to visual attention processes-, and changes in mu and beta oscillations over central scalp locations -associated with sensory and motor functions- (Galdo-Alvarez et al., 2016; González-Villar et al., 2016; Huster et al., 2013; Wagner et al., 2018). In addition, fast bursts in the beta range over the right frontal cortex- associated with the activation of a fronto-basal ganglia inhibitory network- are also a common neural correlate of motor inhibition (Jana et al., 2020; Wessel, 2020).

There are some inherent problems when interpreting ERP data obtained from the classical SST. The comparison of Go versus Stop trials entails difficulties since the brain electrical activity evoked by the Go and Stop signals overlap within the Stop trials, and because both types of trials differ in their frequency. This design also causes problems in the baseline correction, given that the Stop signal is typically presented at variable delays (Ramautar et al., 2004), and makes it difficult to separate sensory- versus inhibitory-related brain activity, appearing at similar latencies and topographies (González-Villar et al., 2016). In addition, the SST may lack ecological validity. In real contexts, not all unexpected events require stopping the ongoing action; furthermore, stimuli that require stopping or continuing an action can be very similar (e.g., a policeman indicating that we have to stop or continue). Nevertheless, in the classical SST, the unpredictable stimuli are always signals that require inhibition, while the brain activity evoked by unforeseen signals that require continuing the response has been poorly studied.

To better understand if signals with different meaning (but similar physical characteristics) activate analogous brain networks, while trying to overcome the methodological difficulties surrounding the classical SST, we recorded the EEG during a modified SST. The task included 3 types of trials: Only Go signal (Go; white arrow); Go signal followed by a confirmation signal (herein named CGo; white arrow + green arrow); Go signal followed by a Stop signal (Stop; white arrow + red arrow). To isolate the role of actual motor output, the task was performed during overt execution and mental rehearsal (participants had to imagine responding or inhibiting the response). We compared ERPs and EEG time-frequency data obtained in the three types of trials in overt and imagined conditions. Finally, to clarify to what extent the EEG activity evoked by infrequent signals that may require either stopping or continuing the action are distinctive, we applied a machine learning technique to classify EEG data evoked by Stop versus CGo trials during overt and imagined execution.

We predicted larger N2 and P3 amplitudes and midfrontal theta power modulation in Stop trials than in CGo or Go trials (and no differences between the latter), as well as lower brain activity modulation and reduced differences among the conditions in the mental rehearsal task. Finally, we expected to accurately classify brain signals evoked by Stop and CGo trials using machine learning algorithms, both in overt and imagined execution.

Our findings will clarify whether the brain activity commonly related to motor inhibition (N2, P3, and midfrontal theta power) is specific to Stop signals or is also evoked by infrequent signals that do not require inhibition. Also, the results of applying machine learning procedures will contribute to clarify whether the EEG data during imagined performance contain useful information to discriminate between trials that require stopping or continuing the action.

2 | METHOD

2.1 | Participants

Twenty-three volunteer students (all women) from the University of Santiago de Compostela, with an age range of 20–24 years (mean = 20.58; SD = 1.057) participated in the study. All reported having normal or corrected vision with glasses or contact lenses. Twenty participants were right-handed according to Edinburgh's Manual Preference Inventory (Oldfield, 1971). None of the participants had a history of psychiatric or neurological illness or substance abuse.

2.2 | Stimuli and procedure

Participants were comfortably seated in an armchair and tested in a dimly lit, sound-attenuated room. The tasks were designed and presented with the STIM program (Neuroscan Labs) in a 15-inch screen located at a distance of 100 cm from the participant' eyes. The stimuli consisted of an arrowhead and a tail and had a size of 2.1° x 1.4° of visual angle presented on a black background. Participants had to respond using a response box that they hold with their hands. The primary task consisted in white arrows pointing to the left (50%) or to the right (50%). In some trials, the initial white arrow could change unpredictably to red or green after a variable interval. The red arrow was a Stop signal, indicating to stop the already prepared or initiated response; the green arrow was a confirmation signal, indicating that the response should be emitted. Both stimuli (the red and green arrows) had a luminance of 75 lux. The task had 400 trials, 260 Go only trials (65%), 60 CGo trials (15%), and 80 Stop trials (20%). The inter-trial interval had a random value between 2100 ms and 2400 ms. For CGo and Stop trials, the second arrow had a delay of 166 ms (10 frames in a 60 Hz refresh rate monitor), 233 ms (14 frames), or 300 ms (18 frames) after the initial Go signal. The delays were randomly selected and were equiprobable. The arrows had a total duration of 500 ms (See Figure 1a). A training block was carried out at the beginning of the experiment.

The task was performed twice, first in overt execution and then in an imagined condition, with a 5-minute break in-between. Tasks were not counterbalanced as prior reports revealed that covert motor performance benefits from overt motor practice (Carrillo-de-la-Peña et al., 2006; Cunnington et al., 1996). The task with imagined performance had the same parameters as the task with overt performance. During the imagined condition, participants were instructed to imagine the execution of the action as vividly as possible (they should imagine themselves pressing the button after the white or green arrows and stopping the response after the red arrow), while they kept their hands on the response box without making any movement.

2.3 | Psychophysiological recording and ERP analyses

EEG was recorded with a Neuroscan equipment (NeuroScan Labs, SynAmps Model 5083 amplifier) by 28 Ag/AgCl electrodes positioned using the 10–20 international system, and referenced to the left and right mastoids. The electrooculogram (EOG) was recorded from sites above and below the left eye and from electrodes lateral to each eye. The AFz electrode was used as ground. Impedances were kept below 10 kΩ. The EEG signals were digitized at a rate of 500 Hz with a Neuroscan equipment (Neuroscan Laboratories, version 4.1), and filtered online using a band-pass filter between 0.1 and 100 Hz and a notch filter of 50 Hz. The EEG was resampled to 250 Hz and filtered using a band pass FIR filter from 0.1 Hz to 40 Hz, as implemented in "pop_eegfiltnew" Eeglab function –filter order of 8250 for 0.1 Hz and 84 for 40 Hz-. Epochs from −800 ms to 1800 ms were extracted time-locked to the events. Baseline correction was applied from −200 ms to 0 ms for epochs time-locked to Go signals, and from −500 to −300 for epochs time-locked to CGo and Stop signals. This different baseline interval for CGo and Stop epochs was selected to minimize the effect of the preceding Go signal. Note that averaged Stop epochs included trials with both successful and unsuccessful inhibitions. For Go, CGo, and unsuccessful inhibition conditions, only trials in which the direction of the arrow was correctly responded to were included. Epochs were linearly detrended using Matlab's "detrend" function, and noisy epochs were rejected manually after visual inspection. Electrodes with high noise levels were removed and reconstructed using spherical splines interpolation. In the overt condition, a total of 27 electrodes were interpolated; for the imagined condition, it was a total of 18. Extended Independent Component Analysis was applied to remove artifacts. Noisy components were first marked using MARA software (Winkler et al., 2014), and then removed after visual confirmation.

To ensure that no actual response was made during the imagined task, we recorded the electromyography (EMG) with bipolar electrodes placed on the ventral side of each forearm, trisecting the wrist–elbow distance (to record the activity of the flexor digitorum profundis, the flexor digitorum superficialis, and the flexor pollicis longus of both arms). To remove epochs with high EMG activity, we computed the root mean squared (RMS) of both EMG channels (left and right arm). Epochs that contained maximum RMS values during the poststimulus interval (from 200 ms to 1000 ms for Go, and from −200 ms to 600 ms for CGo and Stop trials) that were 3 times higher than the maximum value in baseline period (from −200 ms to 0 ms for Go, and from −500 ms to −300 ms for CGo and Stop trials) were rejected (See Figure 3d). With this procedure, a mean of 7.7 ± 11% of the Go epochs, 7.1 ± 10% of the CGo, and 3.4 ± 4.8% of the Stop epochs were rejected. After the different data cleaning steps, the following mean number of epochs remained for further analysis: Overt Go = 235.3 ± 19.5 epochs; Overt CGo = 53.2 ± 5.2 epochs; Overt

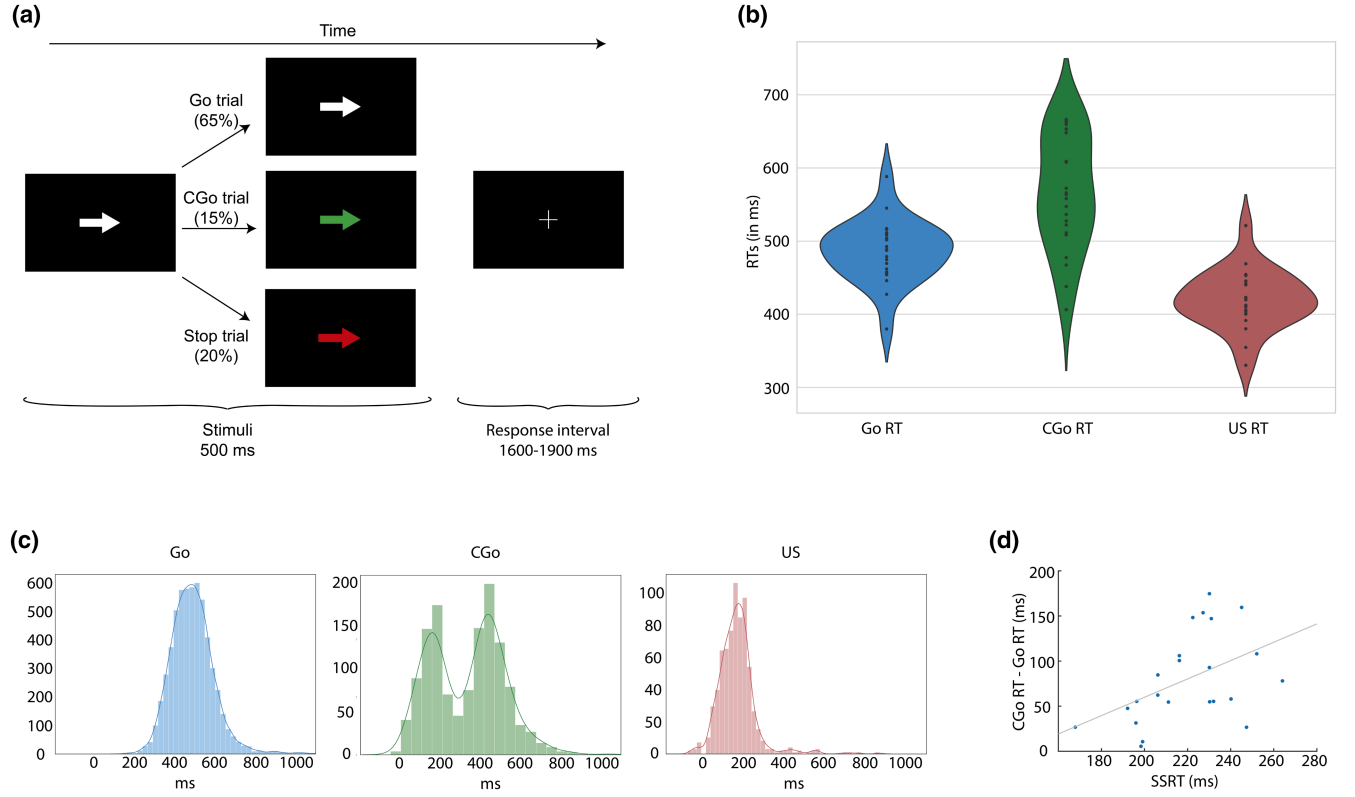

FIGURE 1 (a) Task description. (b) Violin plots of the mean reaction times (RTs) for each condition with behavioral response: Go; confirmatory Go (CGo) and unsuccessfully stopped trials (US). These mean reaction times were measured from the presentation of the first Go arrow. (c) Histograms showing all the single reaction times (gathering all the trials and all the participants) in each one of the three conditions with responses. Histograms for the CGo and Stop conditions are time-locked to the presentation of the second arrow. Green histogram shows that in the CGo condition there is a much lower amount of responses around 300 ms after the presentation of the confirmatory signal. (d) Scatter plot. The x-axis shows the stop-signal reaction time (SSRT), and the y-axis shows the subtraction of reaction times of the CGo minus Go trials. A positive correlation between the two indices can be observed

Stop = 72.6 ± 5.7 epochs; Imagined Go = 219.9 ± 30.7 epochs; Imagined CGo = 50.7 ± 6.5 epochs; Imagined Stop = 70.5 ± 7.4 epochs. Finally, we measured the amplitudes of the N2 and P3 components for their analysis (see the "Statistical analysis" section).

2.4 | Time-frequency analysis

Time-frequency analysis was performed by convolving the EEG data with a family of complex Morlet wavelets ranging in frequency from 2 to 35 Hz in 30 logarithmically increasing steps, and with logarithmically increasing cycles, from 3 cycles at the lowest frequency to 8 at the highest frequency. Power data obtained after convolution was baseline corrected by transforming the power change of each time-frequency pixel to dB, relative to the mean power in the baseline interval of each frequency. The baseline interval was from −500 to −300 ms when the analysis was performed time-locked to the first arrow (Go trials), and from −600 to −400 when it was time-locked to the second arrow (CGo or Stop trials). Midfrontal theta power was measured for later analysis (further details are given in the "Statistical analysis" section).

2.5 | Machine learning classification

To determine if brain signals contain information about the inhibitory meaning of the stimuli, and not only about their salience, we used an approach similar to that used in previous studies (Bae & Luck, 2018; Foster et al., 2017). To increase the signal-to-noise ratio, trials in each condition (CGo and Stop) were randomly divided into three parts (using the same number of epochs in each third for each condition, determined by the condition with the lowest number of trials), and then averaged them, obtaining three different ERPs for each condition. Subsequently, 2/3 ERPs (in each condition) were used to train the algorithm, and the remaining 1/3 was used for prediction. This was repeated 3 times, using a different 1/3 for the prediction (threefold cross-validation). The decoding procedure, performed for each time-point, and using the 28 scalp electrodes, was

repeated 200 times, with different epochs randomly assigned to the three bins (2 prediction and 1 test) in each iteration. Machine learning classification was done with a support vector machine algorithm (SVM) in Matlab, using a code adapted from Bae and Luck (2019). Given that this is a binary classification (either CGo or Stop trial) the chance performance was 50%. For the training of the SVM we used the "fitcsvm" Matlab function. For each participant, the decoding accuracy was temporally smoothed with a centered moving average by sliding a window of five time-points length, using the Matlab function "movmean."

2.6 | Statistical analysis

Repeated measures ANOVAs with condition (type of trial) as within-subject factor were used to analyze behavioral (reaction times) and electrophysiological data (N2, P3, theta power), for each task (overt vs. imagined) separately. The selection of different electrodes and time windows was based on both previous literature and visual inspection. The N2 component showed its maximum amplitude from 200 to 300 ms over frontocentral locations (FCz electrode), while P3 showed its maximum amplitude from 300 to 500 ms at centro-parietal locations. Given that the Stop-P3 is commonly measured in the Cz electrode, here we also used this location. Differences in mean amplitudes in these windows and locations were tested for significance using the ANOVAs. In addition, since the amplitude of the ERPs was lower in the imagined condition –and thus the mean amplitude could be less sensitive to condition differences in this task-, we also measured the peak amplitude of N2 and P3 for a complementary analysis. Theta power was measured in the time window, frequencies, and location where it peaked (from 200 ms to 450 ms, 3.5–7 Hz, and at the FCz electrode).

Finally, to clarify whether there were any task differences (overt vs. imagined) in the measured indexes (N2, P3, and theta), comparisons between tasks (overt vs. imagined) were made using repeated measures ANOVAs.

Post hoc paired t tests were used to evaluate significant differences, with Holm adjustment for multiple comparisons (Holm, 1979).

In addition to frequentist statistics, we also report results from Bayesian statistics. Both statistical approaches were conducted using JASP 0.14.1 software. For the Bayesian ANOVA alternative we used a prior for fixed effects = 0.5; while for the Bayesian t test, we used a default Cauchy prior with a scale value of 0.707. A common way to interpret the reported Bayes Factors (BF_{10}) is using the categorization proposed by Lee and Wagenmakers (2013). In this classification BF_{10} between 1 and 3 are labeled as "anecdotal evidence" in favor of the alternative hypothesis, between 3 and 10 as "moderate evidence", between 10 and 30 as "strong evidence", between 30 and 100 as " very strong evidence", and larger BFs as "extreme evidence" in favor of the alternative hypothesis. Conversely, values between 1 and 1/3 are labeled as "anecdotal evidence" in favor of the null hypothesis, between 1/3 and 1/10 as "moderate evidence", between 1/10 and 1/30 as "strong evidence", and so on.

To evaluate if the decoding accuracy was above chance, we used a cluster-based permutation approach as described in Bae and Luck's (2019) work. First, a one-tailed, one-sample t test was performed for each time point (81 time points, from −400 to 1200 ms) in the observed data. We then extracted the clusters of contiguous time points for which the p values were $< .001$, and summed the total t values of each cluster (t mass values). To determine whether a cluster was larger than the expected by chance, the data were permuted 1000 times. In each permutation the target labels (CGo or Stop) were shuffled. To account for temporal auto-correlation of the EEG data, the same target labels were used for all the time points in each epoch. As in the original calculation of the decoding accuracy, the decoding accuracy for permutations was also repeated 600 times (3 times [using a different 1/3 for the prediction] *200 iterations). Again, for each permutation the averaged decoding accuracy values were smoothed across time using a five-point moving window. The cluster with the highest t mass was saved in each permutation. The p value of a cluster was calculated by the position of the observed t mass value in the ordered t mass values of the permutations. A cluster was considered significant if it had a t mass value above the 99% of the null distribution. We report $p < .001$ if the observed cluster had a t mass value higher than the 1000 clusters obtained during permutations. In addition, for descriptive purposes, we also report the t values and p values of a one-tailed one-sample *t* test of the mean accuracy in the cluster that was detected as significant after permutation testing. This procedure was independently performed for the overt and for the imagined tasks.

3 | RESULTS

3.1 | Behavioral results

During the overt task participants had a 96.3% of correct responses in Go trials, a 94.9% in CGo trials, and a 61.7% of correct inhibitions in Stop trials. We performed an ANOVA to assess the effect of condition

(Go, CGo, and unsuccessful Stop [US]) on reaction times (RTs). We found a main effect of condition in RTs (Go = 486 ± 42 ms; CGo = 566 ± 78 ms; US = 420 ± 39 ms; $F_{[2,44]} = 127$; $p < .001$; $BF_{10} = 2.23e16$). Post hoc paired comparisons with Holm correction showed significant differences between the three measures ($p < .001$ in all cases), with the faster reaction times for the US trials, followed by the Go trials, and the slowest for the CGo trials (See Figure 1b). Figure 1c shows the histograms using the single reaction times from all the trials and participants; it can be observed that in contrast to the other conditions, the CGo condition shows a bimodal distribution, with a noticeable decrease in the total number of responses at around 300 ms after the presentation of the CGo arrow, which suggests that the CGo signal produces an interference observed in the behavior after 300 ms. Supplementary Figure S1 (Section A) shows that this decrease in the number of responses after 300 ms is observed in each of the signal delays used (i.e., 166, 233 or 300 ms between Go and CGo arrows). Supplementary Figure S1 (Section B) shows the proportion of US trials for each participant.

The mean stop-signal delay (the time between presentation of the Go signal and presentation of the stop signal) was 232 ± 0.9 ms. The Stop-signal reaction time (SSRT), computed using the integration method (Verbruggen et al., 2019), was 220 ± 23 ms. To further explore whether there is a relation between the SSRT and the interference produced by the CGo signal, we conducted a post hoc analysis by calculating the Pearson correlation between the SSRT and the difference CGo RT minus Go RT. We found that the indexes were positively correlated (r = 0.46; $p = .026$) (See Figure 1d), suggesting that the time required to inhibit an undesired response is related to the interference produced by an unpredicted confirmatory signal, and that both indices may be reflecting the functioning of similar mechanisms.

3.2 | Brain electrical activity during the overt SST

Figure 2 shows the ERPs and time-frequency decompositions for each condition during overt execution. It can be observed that similar waveforms and topographies are evoked during CGo and Stop trials, although the ERP components show larger amplitude in the stop condition.

We first performed an ANOVA on the N2 mean amplitude from 200 to 300 ms at the FCz electrode, comparing Go,

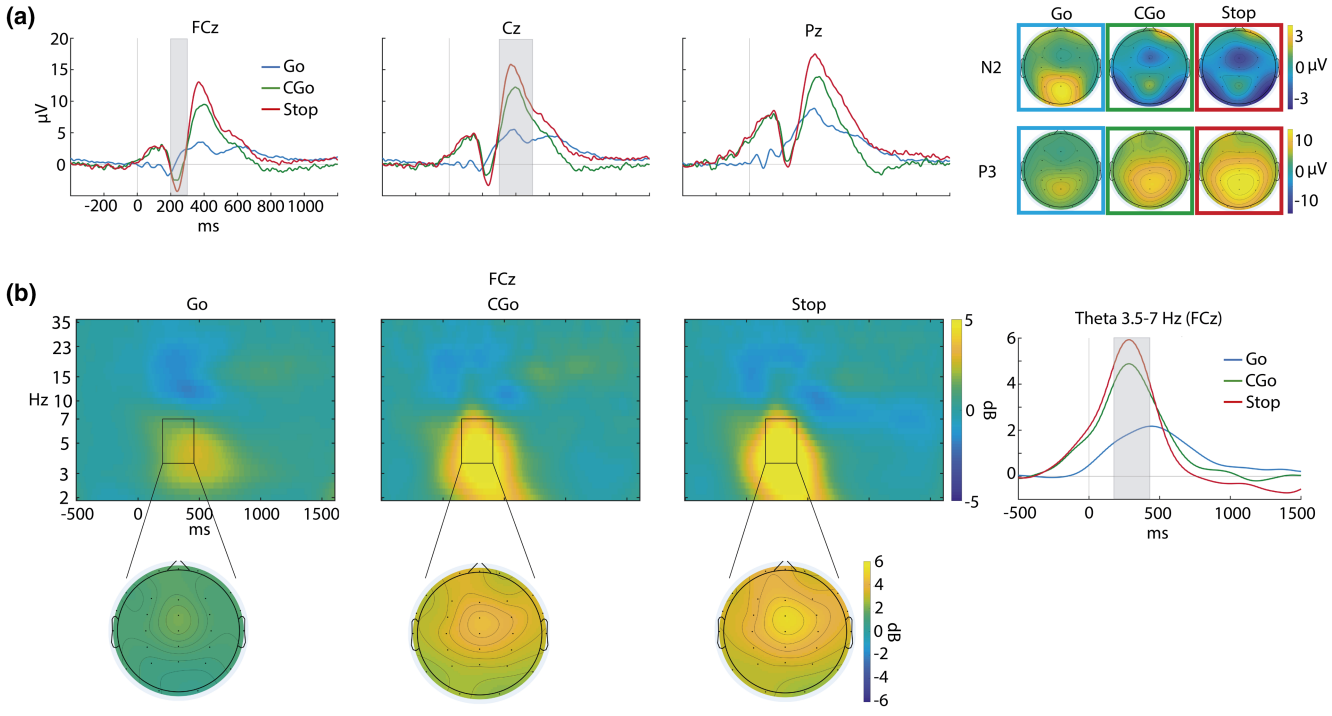

FIGURE 2 (a) Event-related potentials for Go, confirmatory Go (CGo), and Stop trials at the FCz, Cz, and Pz electrodes; shaded areas show the windows used to compute the mean amplitude for each component. Right column shows the topographies of N2 and P3 for each condition. (b) Time-frequency decomposition for each condition at the FCz electrode. Lower row shows the topographies of theta power (measured in a window from 3.5 to 7 Hz and 200 to 450 ms). On the right-hand side, the time-course of the theta power in each condition is shown (shaded area shows the time window used for statistical analyses)

CGo, and Stop trials. We found a main effect of condition ($F_{[2,44]} = 8.33$; $p = .001$; $BF_{10} = 36.82$). Post hoc paired comparisons with Holm correction showed that the amplitude of this component was significantly higher in Stop than in Go trials ($t_{[22]} = 3.76$; $p = .003$; $BF_{10} = 32.90$), and higher in CGo than in Go trials ($t_{[22]} = 2.54$; $p = .037$; $BF_{10} = 2.94$), but no significant differences were observed between CGo and Stop trials ($t_{[22]} = -1.37$; $p = .18$; $BF_{10} = 0.50$). We also performed a post hoc complementary exploratory analysis by measuring the peak of N2 (the most negative value in a window from 150 to 350 ms in the FCz electrode). Results of peak amplitude were congruent with mean amplitude of N2, and confirmed a main effect of condition ($F_{[2,44]} = 7.77$; $p = .003$; $BF_{10} = 25.26$). Significant pairwise comparisons were also congruent: Go versus CGo ($t_{[22]} = 2.46$; $p = .036$; $BF_{10} = 2.66$) and Go versus Stop ($t_{[22]} = 3.90$; $p < .001$; $BF_{10} = 11.34$), but not CGo versus Stop ($t_{[22]} = 1.44$; $p = .157$; $BF_{10} = 0.99$).

For the P3 wave (measured as the mean amplitude from 300 to 500 ms at the Cz electrode) we also found a main effect of condition ($F_{[2,44]} = 50.38$; $p < .001$; $BF_{10} = 1.42e9$). Post hoc comparisons showed significant differences between conditions in the three pairs: with higher amplitude for Stop than Go trials ($t_{[22]} = -8.69$; $p < .001$; $BF_{10} = 897{,}153.81$), for Stop than CGo trials ($t_{[22]} = -5.20$; $p < .001$; $BF_{10} = 751.28$), and for CGo than Go trials ($t_{[22]} = -5.73$; $p < .001$; $BF_{10} = 2357.40$). Here, we also performed a post hoc complementary analysis measuring P3 peak amplitude as the maximum value from 250 to 600 ms in the Cz electrode. Again, results were congruent with the ones reported for mean P3 amplitude, both for the main effect ($F_{[2,44]} = 52.14$; $p < .001$; $BF_{10} = 5.92e51$) and for pairwise comparisons: Go versus CGo ($t_{[22]} = -6.75$; $p < .001$; $BF_{10} = 1.26e18$), Go versus Stop ($t_{[22]} = -10.01$; $p < .001$; $BF_{10} = 376{,}950.54$), CGo versus Stop ($t_{[22]} = -3.25$; $p = .002$; $BF_{10} = 4.59e17$).

For the midfrontal theta (measured as the mean power from 3.5 to 7 Hz and from 200 to 450 ms in the FCz electrode) we found a main effect of condition ($F_{[2,44]} = 48.81$; $p < .001$; $BF_{10} = 1.6e8$) (Go = 1.97 ± 1.30 dB; CGo = 4.18 ± 1.98 dB; Stop = 4.88 ± 2.21 dB). Pairwise comparisons showed that theta power was significantly higher for Stop than CGo trials ($t_{[22]} = -2.40$; $p = .021$; $BF_{10} = 2.9$), for Stop than Go trials ($t_{[22]} = -9.50$; $p < .001$; $BF_{10} = 52{,}552.47$), and also for CGo than Go trials ($t_{[22]} = -7.10$; $p < .001$; $BF_{10} = 96{,}055.78$). Comparisons between unsuccessful stop (US) and successful stop (SS) trials in the overt task are reported in the Supplementary Figure S1 (Sections C and D). See also the Supplementary Figure S2 for an exploratory post hoc analysis performed on the time-frequency activity at the beta range.

3.3 | Brain electrical activity during imagined performance of the SST

To assess whether a similar pattern of activity exists during mental rehearsal, we compared ERPs amplitudes and theta power between Go, CGo, and Stop trials while the participants imagined performing the task. Figure 3 (sections a and b) shows the electrophysiological activity during mental rehearsal. It can be observed that, in general, the pattern of activity is similar to that observed during the overt execution.

To measure N2 we used the mean value in a window from 200 to 300 ms over the FCz electrode. We found a main effect of condition ($F_{[2,44]} = 5.04$; $p = .011$; $BF_{10} = 5.80$). Post hoc comparisons showed significant differences between Go and Stop trials, with higher amplitude for the Stop trials ($t_{[22]} = 2.61$; $p = .048$; $BF_{10} = 3.32$), but not between Stop and CGo trials ($t_{[22]} = 2.06$; $p = .10$; $BF_{10} = 1.30$) or between CGo and Go trials ($t_{[22]} = 1.48$; $p = .15$; $BF_{10} = 0.56$). As in the overt condition, and since the amplitudes of the ERPs are smaller during this task and mean window values could be masking some condition differences, we also performed a post hoc complementary analysis by measuring the peak of N2 (the most negative value in a window from 150 to 350 ms in the FCz electrode). Using peak amplitude we found a main effect of condition ($F_{[2,44]} = 4.16$; $p = .022$; $BF_{10} = 2.54$), although post hoc comparisons did not show any difference between conditions (Go vs. CGo ($t_{[22]} = 0.85$; $p = .41$; $BF_{10} = 0.30$); Go vs. Stop ($t_{[22]} = 2.15$; $p = .13$; $BF_{10} = 1.5$); CGo vs. Stop ($t_{[22]} = 2.13$; $p = .14$; $BF_{10} = 1.43$)).

For the P3 wave –using the mean value in a window from 300 to 500 ms– we found a main effect of condition ($F_{[2,44]} = 3.39$; $p = .043$; BF10 = 1.43), without significant differences in the pairwise contrasts (Go vs. CGo ($t_{[22]} = -1.09$; $p = .29$; $BF_{10} = 0.37$); Go vs. Stop ($t_{[22]} = -2.29$; $p = .10$; $BF_{10} = 1.89$); CGo vs. Stop ($t_{[22]} = -1.65$; $p = .23$; $BF_{10} = 0.70$)). We also measured the P3 peak amplitude as the maximum value from 250 to 600 ms in the Cz electrode. We found a main effect of condition ($F_{[2,44]} = 7.84$; $p = .001$; $BF_{10} = 26.83$); post hoc comparisons showed higher amplitude for Stop than Go trials ($t_{[22]} = -3.72$; $p = .004$; $BF_{10} = 17.99$), and no significant differences between Go and CGo trials ($t_{[22]} = -2.40$; $p = .051$; $BF_{10} = 2.27$) nor between CGo and Stop trials ($t_{[22]} = -1.69$; $p = .105$; $BF_{10} = 0.44$).

For the midfrontal theta (measured as the mean power from 3.5 to 7 Hz and from 200 to 450 ms in the FCz electrode) we found a main effect of condition ($F_{[2,44]} = 22.04$; $p < .001$; $BF_{10} = 51{,}241.89$) (Go = 0.90 ± 0.84 dB; CGo = 1.84 ± 1.54 dB; Stop = 2.73 ± 2.17 dB). Pairwise comparisons showed higher power for Stop than for

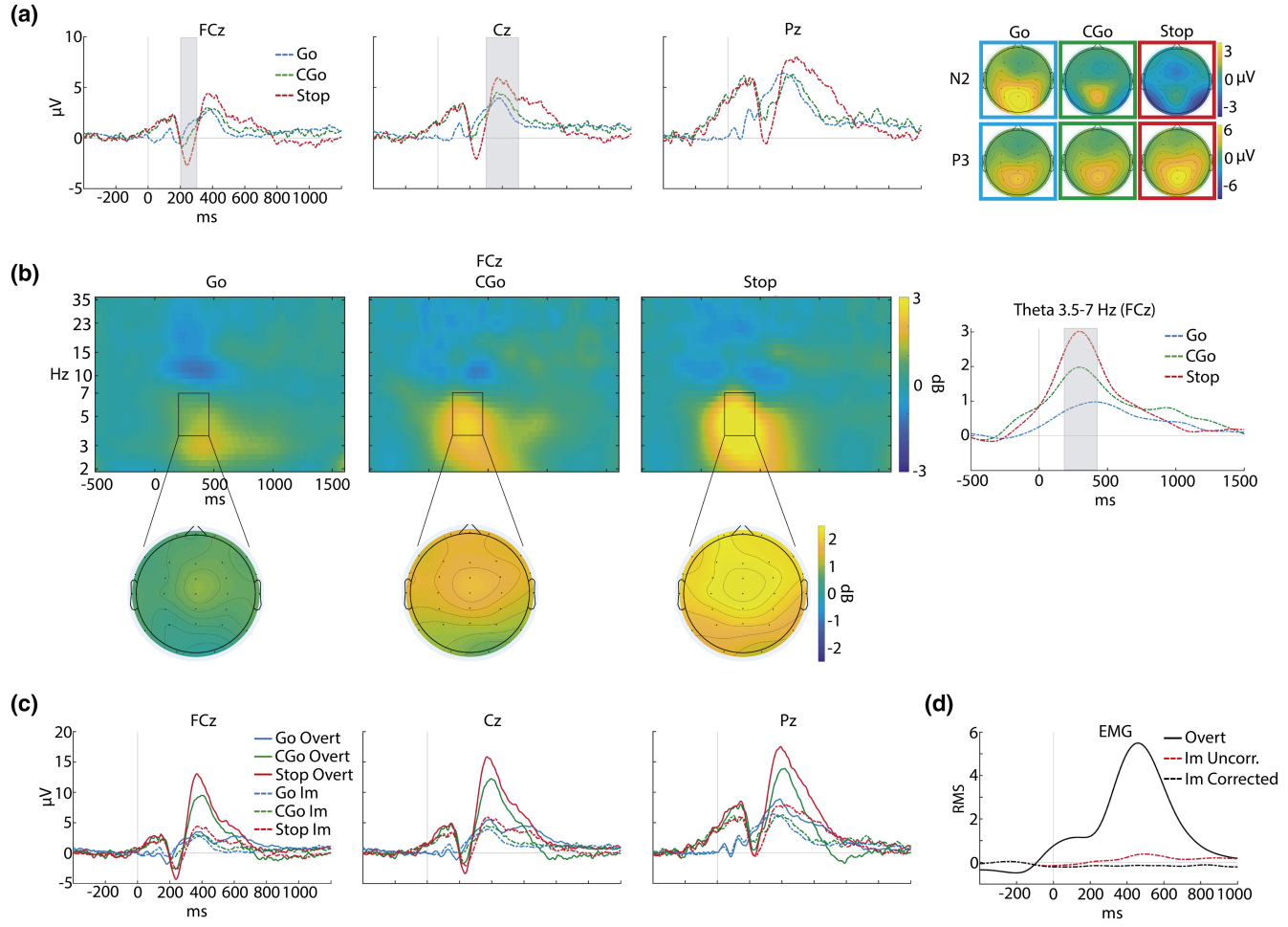

FIGURE 3 (a) Event-related potentials for Go, confirmatory Go (CGo), and Stop trials at the FCz, Cz and Pz electrodes during the imagined task. The topographies of the N2 and P3 components are shown on the right-hand side. (b) Time-frequency decomposition for each condition in the FCz electrode during the imagined task. Lower row shows the topographies of theta power (measured in a window from 3.5 to 7 Hz and 200 to 450 ms). Right column shows the time course of theta power (the shaded area indicates the time window used for the statistical comparison). (c) ERPs comparing go, CGo and stop trials during overt and imagined tasks tasks. (d) Root mean squared (RMS) electromyographic activity of the responding hand (averaging go, CGo, and stop epochs) for the overt task, and the imagined task before (dashed red line) and after (dashed black line) the elimination of the epochs with muscular activity

CGo ($t_{[22]} = -3.24$; $p = .003$; $BF_{10} = 72.89$) and Go trials ($t_{[22]} = -6.64$; $p < .001$; $BF_{10} = 429.40$), and for CGo than for Go trials ($t_{[22]} = -3.39$; $p = .003$; $BF_{10} = 147.74$).

3.4 | Brain activity in overt versus imagined performance

To verify that the amplitude and power modulation of brain activity is lower during mental rehearsal, we also compared electrophysiological indices between overt and imagined tasks (see Figure 3c). We performed a repeated-measures ANOVA to assess the effect of task (including Go, CGo, and Stop trials). For the N2 component (FCz electrode in a window from 150 to 350 ms), no task differences were observed using the mean window amplitude ($F_{[1,22]} = .46$; $p = .5$; $BF_{10} = 0.56$), but a significant main effect of task appeared using N2 peak amplitude data ($F_{[1,22]} = 5.99$; $p = .023$; $BF_{10} = 9.39$), with higher amplitudes for this component during the overt condition. Differences were observed in the same direction using either the mean amplitude of P3 ($F_{[1,22]} = 25.63$; $p < .001$; $BF_{10} = 2778.27$) or the maximum peak of P3 ($F_{[2,44]} = 26.02$; $p < .001$; $BF_{10} = 81{,}528.29$), with higher values in the overt SST. Finally, theta power was significantly higher for the overt task ($F_{[1,22]} = 88.24$; $p < .001$; $BF_{10} = 7.5e7$). EMG activity in each task is depicted in Figure 3d.

3.5 | Classification between CGo and stop trials using brain activity data

Finally, we tested if decoding accuracy between CGo and Stop epochs using a SVM algorithm was above chance

level in both, overt and imagined tasks. For the overt task, permutation testing found a significant cluster ($p < .001$) at a time-range from 120 to 1200 ms. The one-tailed t test for the mean value of this cluster was $t_{(32)} = 18.63$; $p < .001$. For the imagined task, permutation testing found a significant cluster ($p < .001$) from 120 to 760 ms. The one-tailed t test in the mean accuracy value of this cluster was $t_{(32)} = 19.98$; $p < .001$. Figure 4 shows the decoding accuracy at each time point during both tasks. It can be seen that accuracy decays after 600 ms in the imagined task, while it is maintained for longer in the overt task.

4 | DISCUSSION

To better understand the brain activity associated to inhibitory processes, in the current study we used a modified version of the Stop-signal task (SST) with confirmatory Go signals (CGo) presented unpredictably after Go signals. Our results showed that unpredictable CGo nonStop signals also cause inhibition as evidenced by longer RTs and similar brain electrical activity, although with smaller amplitude to the one evoked by the Stop signals. This pattern of activity was also reproduced during mental rehearsal of the task. In addition, we found that the brain activity linked to the unpredictable CGo versus Stop signals can be classified above chance using machine learning algorithms, both in overt and imagined performance.

During the overt task, we found that the presentation of CGo signals slowed down reaction times, in comparison to Go signals presented alone. Previous studies found motor slowing associated to Go signals in selective stopping tasks that require to inhibit only a part of the response (Macdonald et al., 2012), and also after execution errors (Danielmeier & Ullsperger, 2011; Li et al., 2008). Here, we found that motor slowing can also occur after unpredictable infrequent signals, even if they confirm that the behavior is being correctly executed. This effect is clearly illustrated in Figure 1, where there is a marked reduction in the total number of responses at around 300 ms after the CGo signal (green histogram), and supports recent research that found the engagement of inhibitory control after the presentation of infrequent signals (Iacullo et al., 2020; Waller et al., 2019). The slowing after CGo signals suggest that the engagement of the *hyperdirect inhibitory pathway* (Hamani et al., 2017) and the interruption of ongoing actions may happen before, or in parallel, to the full extraction of the meaning of the unpredictable signal. This idea is in line with the theory that surprise is accompanied by automatically engaged motor inhibition (Iacullo et al., 2020; Wessel & Aron, 2017); and also with the model "pause-then-cancel" which proposes that inhibition occurs in two steps. A first step, "pause", which is initially activated after the presentation of surprising stimuli; and a second step, "cancel" (or continue for the case of CGo signals), that occurs after further evaluation of the stimuli (Schmidt & Berke, 2017; Tatz et al., 2021).

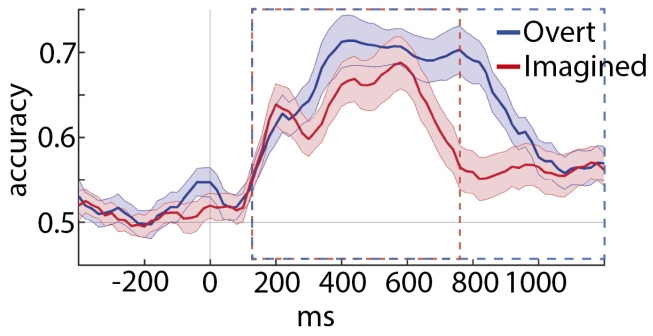

FIGURE 4 Decoding accuracy between CGo and stop trials at each time point during overt and imagined tasks. Bounded areas show the standard error of the mean. Boxes show clusters with significant differences above chance during overt (blue line) and imagined execution (red line)

We also found that the slowing caused by CGo signals (computed as the difference in RTs to CGo minus Go trials) was correlated with the Stop-signal reaction time (SSRT). This finding suggests that the index (CGo RT-Go RT) may be a potential marker of the integrity of inhibitory networks which complements the SSRT index, since it probably reflects processes more related to an unintended and automatic inhibitory interference.

In line with the behavioral results, we observed that the electrical brain activity evoked by CGo trials had a similar topographic distribution to the one evoked by Stop signals––both elicited midfrontal N2 and P3 components and midfrontal theta power increase. N2 has been related to the detection of a conflict between the Go and no-Go signals or between the Go and Stop signals (Donkers & Van Boxtel, 2004; Nieuwenhuis et al., 2003). We found that the N2 was higher for Stop and CGo than for Go signals. Since CGo signals reinforce the response being executed and thus are not conflicting, the larger N2 in CGo than in Go trials suggests that this component should not be interpreted exclusively in terms of conflict detection; it may be also reflecting attentional orienting to a salient or unpredicted stimulus. Similar conclusions can be drawn from the midfrontal theta results, which showed largest power increase in the Stop condition, followed by the CGo condition (in both, real and imagined tasks). Midfrontal theta is functionally related to N2, and has been related to conflict detection and the need for cognitive control (Cavanagh & Frank, 2014). Altogether, our findings suggest that neural correlates classically related with conflict detection are, to some extent, automatically engaged after nonconflictive CGo trials.

Regarding P3, we found that CGo trials elicited a P3 component with similar topographic distribution, but smaller amplitude, than Stop-P3. This finding indicates that, although P3 may partly reflect the processing of a second signal (confirmation or stop), this does not give full account of the difference found across conditions. The neural origins of Stop-P3 are believed to be in areas like the middle cingulate cortex or the inferior frontal cortex (Huster et al., 2010; Rubia et al., 2007; Schall et al., 2002), and this component usually shows greater amplitude when the response is correctly inhibited (Dimoska et al., 2003), supporting its role in the inhibition process. Our result of P3 in unpredictable CGo trials suggests the automatic engagement of the inhibitory cascade, although to a smaller degree than in Stop signals. Thus, ERP components previously interpreted as Stop-related activity are not exclusively elicited by Stop signals, but also appear after stimuli that do not require inhibition nor are in conflict with the ongoing motor plan.

Previous studies showed that unexpected/irrelevant salient stimuli trigger bottom-up processes likely related to the orientation response –and cause an involuntary motor interference (Dimoska et al., 2006; Novembre et al., 2018; Waller et al., 2019; Wessel & Aron, 2017), that has been interpreted as evidence of the activation of inhibitory networks (Wessel & Aron, 2013, 2017; Wessel et al., 2016). Here, we found that also expected stimuli (although infrequent or unpredictable) that explicitly indicate continuing the ongoing action lead to motor slowing (evidenced by slower RTs for the CGo trials) and the activation of motor inhibition networks (suggested by the higher N2 and P3 amplitudes and theta power for CGo than Go trials in the overt task). Thus, our observation suggests that CGo and Stop signals may activate overlapped neural networks, which may be driven by both, bottom-up (i.e., automatic inhibition in the face of a new signal) and top-down processes (i.e., detection of the meaning of the red arrow and activation of inhibitory mechanisms).

There is an ongoing debate about the existence of a specific inhibitory network (involving areas like the right Inferior Frontal Cortex, rIFC) versus a globalist account, which suggests that such areas are part of the multi-demand cortex (MDC) and involved in several control processes (Aron et al., 2015; Hampshire & Sharp, 2015). Sharp et al. (2010) found similar fMRI activation over the rIFC in either CGo or Stop trials, concluding that this area is not inhibition specific, but related to attentional detection. The advocates of the specificity of rIFC in stopping argued that the CGo signals do engage inhibition for being salient, infrequent or unexpected (Aron et al., 2014), while the proponents of the MDC hypothesis rejected this presumption arguing that CGo stimuli are not surprising as they occur on a substantial percentage of trials (Hampshire & Sharp, 2015). Our behavioral and EEG data support the idea that infrequent CGo signals also cause the activation––at least partially––of inhibition processes, and thus provide arguments for the advocates of the specificity hypothesis.

In recent years, much effort has been devoted to the development of brain-computer interface (BCI) devices. These systems are largely based on the hypothesis that brain activity during mental rehearsal is similar to that during overt execution (Jeannerod, 2001). Previous research found a substantial overlap of brain activation during real and simulated execution and inhibition, with weaker neural recruitment during mental rehearsal (Carrillo-de-la-Peña et al., 2008; Galdo-Alvarez et al., 2016; González-Villar et al., 2016). We studied ERPs and time frequency activity associated to CGo and Stop signals during the imagined execution of the modified SST and found similar modulation of brain activity by trial type in the covert task (See Figure 3c). Nevertheless, the differences across conditions were smaller than in the overt task, being the comparison between CGo and Stop trials only significant for theta power, and not for the ERPs. This finding suggests that theta power may be a more sensitive index of conflict detection/inhibition than the N2 and P3 components.

Effective BCI systems need to decode the different brain signals and identify which function each one corresponds to. Here, we found that brain activity evoked by signals that demand totally opposite responses (continue or stopping) can be very similar, as evidenced by ERPs data. Nevertheless, we demonstrated that EEG signals contain decodable information about the inhibitory meaning––and not only about bottom-up stimulus salience––during both overt execution and mental rehearsal of the SST. This decoding accuracy was above chance from 120 ms, showing a local maximum at 200 ms, coincident with the N2 component. However, its highest classification accuracy was between 400 ms and 600 ms, coincident with the P3 component. This observation is in accordance with a recent study using multivariate pattern analysis, that found that ERPs evoked by Stop signal could be decoded from "ignore" signals (analogous to our CGo signals) from 180 ms after signal onset, although better classification accuracy was observed at P3 latencies (Tatz et al., 2021). Finally, an interesting finding is that the peak in decoding accuracy in the imagined condition reached levels similar to those observed in the overt condition, suggesting that the ability to discriminate between CGo and Stop EEG signals is also maintained in mental rehearsal. Thus, our findings suggest that brain indices related to motor stopping can be differentiated from indices evoked by other infrequent stimuli from N2 latencies, but the accuracy is better at P3 latencies. This information is decodable during both overt and imagined performance, and can be potentially applied in the control of BCI systems.

5 | LIMITATIONS

One limitation in the present study was that CGo trials had less probability of appearance than Stop trials. (0.15 vs. 0.2, respectively). This higher number of Stop than CGo trials was due to the objective of achieving a good signal-to-noise ratio to also obtain ERPs for the succesfully stopped (SS) and unsuccesfully stopped (US) trials. Although we do not know to what extent participants were aware of this difference, we performed exploratory analyses of the electrophysiological indices (N2 and P3), and they maintained their differences between conditions both during the first half of the task (when participants should be less aware of the differences in the Stop and CGo ratio) and during the second half (when participants should be more aware of the differences in the ratio).

In addition, in our task the red arrows always represented the need to stop the response, while green arrows represented to continue. It can be argued that since the representation of stop in red color is a culturally learned concept, the use of red arrows triggers greater automatic engagement of inhibitory mechanisms and is responsible of the pattern of results. However, we found that also green arrows cause inhibition and delay in reaction times.

Another limitation is that, due to its simplicity when programming the task, we used three fixed Stop-signal delays presented in a random and equiprobable manner, instead of using methods that are adaptive to the performance of the participants, such as the staircase tracking algorithm. As a result, it was not always possible to obtain probabilities of responding to "Stop" trials at around 0.5 what limits the reliability when computing the SSRT.

Finally, another potential limitation was the order of the tasks (always overt execution followed by mental rehearsal). This may have some fatigue effects, reducing attention levels and presumably causing a reduction in the amplitude of ERPs (Boksem et al., 2005; Kato et al., 2009). Although counterbalancing could help to reduce order effects, we preferred that participants had recent experience in performing the SST to facilitate the execution of the imagined task, in line with previous studies (Carrillo-de-la-Peña et al., 2006; Cunnington et al., 1996).

6 | CONCLUSIONS

The results suggest that the brain activity elicited by unpredictable and infrequent signals requiring opposite responses (either to continue or inhibit the action) can be very similar (producing motor slowing and activation of inhibitory neural networks) but still distinguishable and decodable, even when performed in imagination.

CONFLICT OF INTEREST

The authors declare no conflict of interest.

AUTHOR CONTRIBUTIONS

Alberto J González-Villar: Data curation; investigation; methodology; visualization; writing – original draft; writing – review and editing. **Santiago Galdo-Álvarez:** Conceptualization; formal analysis; methodology; writing – review and editing. **María Teresa Carrillo-de-la-Peña:** Conceptualization; data curation; funding acquisition; project administration; supervision; writing – review and editing.

DATA AVAILABILITY STATEMENT

Data available upon request from the authors.

ORCID

Alberto González-Villar https://orcid.org/0000-0003-0009-920X

REFERENCES

Aron, A. R. (2011). From reactive to proactive and selective control: Developing a richer model for stopping inappropriate responses. *Biological Psychiatry*, *69*(12), e55–e68. https://doi.org/10.1016/j.biopsych.2010.07.024

Aron, A. R., Cai, W., Badre, D., & Robbins, T. W. (2015). Evidence supports specific braking function for inferior PFC. *Trends in Cognitive Sciences*, *19*(12), 711–712. https://doi.org/10.1016/j.tics.2015.09.001

Aron, A. R., Robbins, T. W., & Poldrack, R. A. (2014). Inhibition and the right inferior frontal cortex: One decade on. *Trends in Cognitive Sciences*, *18*(4), 177–185. https://doi.org/10.1016/j.tics.2013.12.003

Bae, G.-Y., & Luck, S. J. (2018). Dissociable decoding of spatial attention and working memory from EEG oscillations and sustained potentials. *The Journal of Neuroscience*, *38*(2), 409–422. https://doi.org/10.1523/JNEUROSCI.2860-17.2017

Bae, G.-Y., & Luck, S. J. (2019). Decoding motion direction using the topography of sustained ERPs and alpha oscillations. *Neuroimage*, *184*, 242–255. https://doi.org/10.1016/j.neuroimage.2018.09.029

Boksem, M. A. S., Meijman, T. F., & Lorist, M. M. (2005). Effects of mental fatigue on attention: An ERP study. *Cognitive Brain Research*, *25*(1), 107–116. https://doi.org/10.1016/j.cogbrainres.2005.04.011

Carrillo-de-la-Peña, M. T., Galdo-Álvarez, S., & Lastra-Barreira, C. (2008). Equivalent is not equal: Primary motor cortex (MI) activation during motor imagery and execution of sequential movements. *Brain Research*, *1226*(mi), 134–143. https://doi.org/10.1016/j.brainres.2008.05.089

Carrillo-de-la-Peña, M. T., Lastra-Barreira, C., & Galdo-Alvarez, S. (2006). Limb (hand vs. foot) and response conflict have similar effects on event-related potentials (ERPs) recorded during motor imagery and overt execution. *The European Journal of Neuroscience*, *24*(2), 635–643. https://doi.org/10.1111/j.1460-9568.2006.04926.x

Cavanagh, J. F., & Frank, M. J. (2014). Frontal theta as a mechanism for cognitive control. *Trends in Cognitive Sciences*, *18*(8), 414–421. https://doi.org/10.1016/j.tics.2014.04.012

Cunnington, R., Iansek, R., Bradshaw, J. L., & Phillips, J. G. (1996). Movement-related potentials associated with movement preparation and motor imagery. *Experimental Brain Research*, *111*(3), 429–436. https://doi.org/10.1007/bf00228732

Danielmeier, C., & Ullsperger, M. (2011). Post-error adjustments. *Frontiers in Psychology*, *2*, 233. https://doi.org/10.3389/fpsyg.2011.00233

Diamond, A. (2013). Executive functions. *Annual Review of Psychology*, *64*, 135–168. https://doi.org/10.1146/annurev-psych-113011-143750

Dimoska, A., Johnstone, S. J., & Barry, R. J. (2006). The auditory-evoked N2 and P3 components in the stop-signal task: Indices of inhibition, response-conflict or error-detection? *Brain and Cognition*, *62*(2), 98–112. https://doi.org/10.1016/j.bandc.2006.03.011

Dimoska, A., Johnstone, S. J., Barry, R. J., & Clarke, A. R. (2003). Inhibitory motor control in children with attention-deficit/hyperactivity disorder: Event-related potentials in the stop-signal paradigm. *Biological Psychiatry*, *54*(12), 1345–1354 Retrieved from http://www.ncbi.nlm.nih.gov/pubmed/14675798

Enriquez-Geppert, S., Konrad, C., Pantev, C., & Huster, R. J. (2010). Conflict and inhibition differentially affect the N200/P300 complex in a combined go/nogo and stop-signal task. *NeuroImage*, *51*(2), 877–887. https://doi.org/10.1016/j.neuroimage.2010.02.043

Foster, J. J., Sutterer, D. W., Serences, J. T., Vogel, E. K., & Awh, E. (2017). Alpha-Band oscillations enable spatially and temporally resolved tracking of covert spatial attention. *Psychological Science*, *28*(7), 929–941. https://doi.org/10.1177/0956797617699167

Galdo-Alvarez, S., Bonilla, F. M., González-Villar, A. J., & Carrillo-de-la-Peña, M. T. (2016). Functional equivalence of imagined vs. real performance of an inhibitory task: An EEG/ERP study. *Frontiers in Human Neuroscience*, *10*(September), 1–12. https://doi.org/10.3389/fnhum.2016.00467

González-Villar, A. J., Bonilla, F. M., & Carrillo-de-la-Peña, M. T. (2016). When the brain simulates stopping: Neural activity recorded during real and imagined stop-signal tasks. *Cognitive, Affective, & Behavioral Neuroscience*, *16*, 825–835. https://doi.org/10.3758/s13415-016-0434-3

Hamani, C., Florence, G., Heinsen, H., Plantinga, B. R., Temel, Y., Uludag, K., Alho, E., Teixeira, M. J., Amaro, E., & Fonoff, E. T. (2017). Subthalamic nucleus deep brain stimulation: Basic concepts and novel perspectives. *ENeuro*, *4*(5). https://doi.org/10.1523/ENEURO.0140-17.2017

Hampshire, A., & Sharp, D. J. (2015). Contrasting network and modular perspectives on inhibitory control. *Trends in Cognitive Sciences*, *19*(8), 445–452. https://doi.org/10.1016/j.tics.2015.06.006

Holm, S. (1979). A simple sequentially rejective multiple test procedure. *Scandinavian Journal of Statistics*, *6*(2), 65–70.

Huster, R. J., Enriquez-Geppert, S., Lavallee, C. F., Falkenstein, M., & Herrmann, C. S. (2013). Electroencephalography of response inhibition tasks: Functional networks and cognitive contributions. *International Journal of Psychophysiology: Official Journal of the International Organization of Psychophysiology*, *87*(3), 217–233. https://doi.org/10.1016/j.ijpsycho.2012.08.001

Huster, R. J., Messel, M. S., Thunberg, C., & Raud, L. (2020). The P300 as marker of inhibitory control – Fact or fiction? *Cortex*, *132*, 334–348. https://doi.org/10.1016/j.cortex.2020.05.021

Huster, R. J., Westerhausen, R., Pantev, C., & Konrad, C. (2010). The role of the cingulate cortex as neural generator of the N200 and P300 in a tactile response inhibition task. *Human Brain Mapping*, *31*(8), 1260–1271. https://doi.org/10.1002/hbm.20933

Iacullo, C., Diesburg, D. A., & Wessel, J. R. (2020). Non-selective inhibition of the motor system following unexpected and expected infrequent events. *Experimental Brain Research*, *238*(12), 2701–2710. https://doi.org/10.1007/s00221-020-05919-3

Jana, S., Hannah, R., Muralidharan, V., & Aron, A. R. (2020). Temporal cascade of frontal, motor and muscle processes underlying human action-stopping. *eLife*, *9*. e50371. https://doi.org/10.7554/eLife.50371

Jeannerod, M. (2001). Neural simulation of action: A unifying mechanism for motor cognition. *Neuroimage*, *14*(1 Pt 2), S103–S109. https://doi.org/10.1006/nimg.2001.0832

Kato, Y., Endo, H., & Kizuka, T. (2009). Mental fatigue and impaired response processes: Event-related brain potentials in a go/nogo task. *International Journal of Psychophysiology*, *72*(2), 204–211. https://doi.org/10.1016/j.ijpsycho.2008.12.008

Lee, M. D., & Wagenmakers, E.-J. (2013). *Bayesian cognitive modeling*. Cambridge University Press. https://doi.org/10.1017/CBO9781139087759

Li, C. R., Huang, C., Yan, P., Paliwal, P., Constable, R. T., & Sinha, R. (2008). Neural correlates of post-error slowing during a stop signal task: A functional magnetic resonance imaging study. *Journal of Cognitive Neuroscience*, *20*(6), 1021–1029. https://doi.org/10.1162/jocn.2008.20071

Macdonald, H. J., Stinear, C. M., & Byblow, W. D. (2012). Uncoupling response inhibition. *Journal of Neurophysiology*, *108*(5), 1492–1500. https://doi.org/10.1152/jn.01184.2011

Novembre, G., Pawar, V. M., Bufacchi, R. J., Kilintari, M., Srinivasan, M., Rothwell, J. C., Haggard, P., & Iannetti, G. D. (2018). Saliency detection as a reactive process: Unexpected sensory events evoke Corticomuscular coupling. *The Journal of Neuroscience*, *38*(9), 2385–2397. https://doi.org/10.1523/JNEUROSCI.2474-17.2017

Oldfield, R. C. (1971). The assessment and analysis of handedness: The Edinburgh inventory. *Neuropsychologia*, *9*(1), 97–113. https://doi.org/10.1016/0028-3932(71)90067-4

Ramautar, J. R., Kok, A., & Ridderinkhof, K. R. (2004). Effects of stop-signal probability in the stop-signal paradigm: The N2/P3 complex further validated. *Brain and Cognition*, *56*(2), 234–252. https://doi.org/10.1016/j.bandc.2004.07.002

Rubia, K., Smith, A. B., Taylor, E., & Brammer, M. (2007). Linear age-correlated functional development of right inferior fronto-striato-cerebellar networks during response inhibition and anterior cingulate during error-related processes. *Human Brain Mapping*, *28*(11), 1163–1177. https://doi.org/10.1002/hbm.20347

Schall, J. D., Stuphorn, V., & Brown, J. W. (2002). Monitoring and control of action by the frontal lobes. *Neuron*, *36*(2), 309–322 Retrieved from http://www.ncbi.nlm.nih.gov/pubmed/12383784

Schmidt, R., & Berke, J. D. (2017). A pause-then-cancel model of stopping: Evidence from basal ganglia neurophysiology. *Philosophical Transactions of the Royal Society B: Biological Sciences*, *372*(1718), 20160202. https://doi.org/10.1098/rstb.2016.0202

Sharp, D. J., Bonnelle, V., De Boissezon, X., Beckmann, C. F., James, S. G., Patel, M. C., & Mehta, M. A. (2010). Distinct frontal systems for response inhibition, attentional capture, and error processing. *Proceedings of the National Academy of Sciences*, *107*(13), 6106–6111. https://doi.org/10.1073/pnas.1000175107

Skippen, P., Fulham, W. R., Michie, P. T., Matzke, D., Heathcote, A., & Karayanidis, F. (2020). Reconsidering electrophysiological markers of response inhibition in light of trigger failures in the stop-signal task. *Psychophysiology*, *57*(10), e13619. https://doi.org/10.1111/psyp.13619

Swick, D., Ashley, V., & Turken, U. (2011). Are the neural correlates of stopping and not going identical? Quantitative meta-analysis of two response inhibition tasks. *Neuroimage*, *56*(3), 1655–1665. https://doi.org/10.1016/j.neuroimage.2011.02.070

Tatz, J. R., Soh, C., & Wessel, J. R. (2021). Common and unique inhibitory control signatures of action-stopping and attentional capture suggest that actions are stopped in two stages. *The Journal of Neuroscience*, *41*(42), 8826–8838. https://doi.org/10.1523/JNEUROSCI.1105-21.2021

van Boxtel, G. J. M. M., van der Molen, M. W., & Jennings, J. R. (2005). Differential involvement of the anterior cingulate cortex in performance monitoring during a stop-signal task. *Journal of Psychophysiology*, *19*(1), 1–10. https://doi.org/10.1027/0269-8803.19.1.1

Verbruggen, F., Aron, A. R., Band, G. P., Beste, C., Bissett, P. G., Brockett, A. T., Brown, J. W., Chamberlain, S. R., Chambers, C. D., Colonius, H., Colzato, L. S., Corneil, B. D., Coxon, J. P., Dupuis, A., Eagle, D. M., Garavan, H., Greenhouse, I., Heathcote, A., Huster, R. J., ... Boehler, C. N. (2019). A consensus guide to capturing the ability to inhibit actions and impulsive behaviors in the stop-signal task. *eLife*, *8*, e46323. https://doi.org/10.7554/eLife.46323

Wagner, J., Wessel, J. R., Ghahremani, A., & Aron, A. R. (2018). Establishing a right frontal Beta signature for stopping action in scalp EEG: Implications for testing inhibitory control in other task contexts. *Journal of Cognitive Neuroscience*, *30*(1), 107–118. https://doi.org/10.1162/jocn_a_01183

Waller, D. A., Hazeltine, E., & Wessel, J. R. (2019). Common neural processes during action-stopping and infrequent stimulus detection: The frontocentral P3 as an index of generic motor inhibition. *International Journal of Psychophysiology*, (January), *163*, 11–21. https://doi.org/10.1016/j.ijpsycho.2019.01.004

Wessel, J. R. (2020). β-Bursts reveal the trial-to-trial dynamics of movement initiation and cancellation. *The Journal of Neuroscience*, *40*(2), 411–423. https://doi.org/10.1523/JNEUROSCI.1887-19.2019

Wessel, J. R., & Aron, A. R. (2013). Unexpected events induce motor slowing via a brain mechanism for action-stopping with global suppressive effects. *The Journal of Neuroscience*, *33*(47), 18481–18491. https://doi.org/10.1523/JNEUROSCI.3456-13.2013

Wessel, J. R., & Aron, A. R. (2015). It's not too late: The onset of the frontocentral P3 indexes successful response inhibition in the stop-signal paradigm. *Psychophysiology*, *52*(4), 472–480. https://doi.org/10.1111/psyp.12374

Wessel, J. R., & Aron, A. R. (2017). On the globality of motor suppression: Unexpected events and their influence on behavior and cognition. *Neuron*, *93*(2), 259–280. https://doi.org/10.1016/j.neuron.2016.12.013

Wessel, J. R., Jenkinson, N., Brittain, J.-S., Voets, S. H. E. M., Aziz, T. Z., & Aron, A. R. (2016). Surprise disrupts cognition via a fronto-basal ganglia suppressive mechanism. *Nature Communications*, *7*, 11195. https://doi.org/10.1038/ncomms11195

Winkler, I., Brandl, S., Horn, F., Waldburger, E., Allefeld, C., & Tangermann, M. (2014). Robust artifactual independent component classification for BCI practitioners. *Journal of Neural Engineering*, *11*(3), 035013. https://doi.org/10.1088/1741-2560/11/3/035013

SUPPORTING INFORMATION

Additional supporting information may be found in the online version of the article at the publisher's website.

FIGURE S1 (a) Histograms showing the single reaction times for the *confirmatory go* (CGo) trials -combining all the trials and all the participants. This figure shows the same data of Figure 1c (green histogram), but split by CGo signal delay. Time= 0 represents the presentation of the CGo signal. A reduction in the total number of responses at around 300 ms after the CGo signal can be observed in the 3 different delays. (b) Boxplot of the proportion of unsuccessful Stop [US] trials in relation to the total Stop trials. Each point represents a single participant. (c) Event-related potentials comparing US and successful Stop [SS] trials during the overt task. Dependent samples t-tests showed significant differences between US and SS trials in N2 mean amplitudes -measured from 200 to 300ms over FCz electrode- ($t_{(22)} = -4.85$; $p < .001$; $BF_{10} = 353.31$); but not in P3 mean amplitudes -measured from 300 to 500ms over Cz electrode- ($t_{(22)} = 0.13$; $p = .9$; $BF_{10} = 0.22$). The topographies of the N2 and P3 components are shown on the right-hand side. (d) Spectrograms of US and SS conditions, including topographies of the theta band between 200 and 500 ms, and the time-course of the theta power on the right-hand side. Dependent samples *t*-tests showed significant differences between US and SS trials in the theta band -measured as the mean power from 200 to 450 ms in the FCz electrode- ($t_{(22)} = 2.36$; $p = .027$; $BF_{10} = 2.14$)

FIGURE S2 Time course of the power in the beta band (from 14 Hz to 24 Hz) over the electrodes in which it showed higher desynchronization (CP3 and CP4) and higher rebound (FCz). Topographic maps show the mean power measured in the area shaded in grey (from 200 ms to 600 ms to measure beta desynchronization and from 800 ms to 1200 ms to measure beta rebound) in each of the 3 trial types. No effect of Condition (Go, CGo, Stop) was found for beta desynchronization during overt ($F_{(1,22)} = 3.05$; $p = .071$; $BF_{10} = 1.11$) or imagined execution ($F_{(1,22)} = 2.07$; $p = .14$; $BF_{10} = 0.56$). There was a main effect of

Condition for the beta rebound during overt performance ($F_{(1,22)}$ = 12.60; p < .001; BF_{10} = 478.82). Post-hoc test showed significant differences between the 3 conditions: Go vs CGo ($t_{(22)}$ = −2.1; p = .042; BF_{10} = 3.61), Go vs Stop ($t_{(22)}$ = 2.9; p = .012; BF_{10} = 4.29); CGo vs Stop ($t_{(22)}$ = 4.99; p < .001; BF_{10} = 145.89). Finally, no differences were observed for beta rebound in the imagined execution ($F_{(1,22)}$ = 0.44; p = .65; BF_{10} = 0.17)

How to cite this article: González-Villar, A., Galdo-Álvarez, S., & Carrillo-de-la-Peña, M. T. (2022). Neural correlates of unpredictable Stop and non-Stop cues in overt and imagined execution. *Psychophysiology*, 59, e14019. https://doi.org/10.1111/psyp.14019